Surface-induced effects in fluctuation-based measurements of single-polymer elasticity: A direct probe of the radius of gyration

Sarah N. Innes-Gold, Ian L. Morgan, and Omar A. Saleh

Citation: The Journal of Chemical Physics **148**, 123314 (2018);
View online: https://doi.org/10.1063/1.5009049
View Table of Contents: http://aip.scitation.org/toc/jcp/148/12
Published by the American Institute of Physics

Surface-induced effects in fluctuation-based measurements of single-polymer elasticity: A direct probe of the radius of gyration

Sarah N. Innes-Gold,[1,a)] Ian L. Morgan,[2,a)] and Omar A. Saleh[1,2,b)]
[1]*Materials Department, University of California, Santa Barbara, California 93106, USA*
[2]*BMSE Program, University of California, Santa Barbara, California 93106, USA*

(Received 12 October 2017; accepted 12 December 2017; published online 29 December 2017)

Single-molecule measurements of polymer elasticity are powerful, direct probes of both biomolecular structure and principles of polymer physics. Recent work has revealed low-force regimes in which biopolymer elasticity is understood through blob-based scaling models. However, the small tensions required to observe these regimes have the potential to create measurement biases, particularly due to the increased interactions of the polymer chain with tethering surfaces. Here, we examine one experimentally observed bias, in which fluctuation-based estimates of elasticity report an unexpectedly low chain compliance. We show that the effect is in good agreement with predictions based on quantifying the exclusion effect of the surface through an image-method calculation of available polymer configurations. The analysis indicates that the effect occurs at an external tension inversely proportional to the polymer's zero-tension radius of gyration. We exploit this to demonstrate a self-consistent scheme for estimating the radius of gyration of the tethered polymer. This is shown in measurements of both hyaluronic acid and poly(ethylene glycol) chains. *Published by AIP Publishing.*
https://doi.org/10.1063/1.5009049

I. INTRODUCTION

The mechanical manipulation of single molecules permits direct insight into polymeric elasticity and, in turn, polymer structure. This methodology has proven quite powerful and broadly applicable, having given insights into the structure of long biopolymers of every type (proteins, polysaccharides, nucleic acids), along with a variety of synthetic polymers. For example, single-molecule stretching has enabled understanding of entropic elastic effects in muscles[1] and permitted the study of solution electrostatic effects in nucleic acids.[2] Theory plays a central role in these advances, particularly as statistical mechanical methods are capable of predicting polymeric force/extension behaviors. Such approaches, in combination with experimental abilities to precisely measure and control force and polymer extension, allow direct, statistically significant comparisons between the model and data, permitting confident validation/negation of polymer structural understanding.

The majority of prior experimental and theoretical work has focused on relatively high-force elastic behavior, with less emphasis placed on understanding low-force elasticity. Low forces are those that permit the chain to loop back on itself, corresponding to forces less than k_BT/ℓ, where ℓ is the chain's Kuhn length and k_BT is the thermal energy.[3] For most flexible biopolymers (e.g., single-stranded nucleic acids, disordered proteins, polysaccharides), ℓ ranges from one to 10 nm, so typical values of k_BT/ℓ are 0.4–4 pN. Such small forces can be reliably controlled by magnetic tweezer manipulation methods[3,4] and are relevant to most biological and biomaterial situations where polymers are frequently under little to no tension.

In the low-force regime, polymers adopt a random walk structure on short length scales, and models based on the classic scaling approaches of polymer physics become appropriate. The key physical metric defining such behavior is typically a power-law exponent. Here, the relevant metric is the Pincus exponent,[5] $\gamma \approx 2/3$, which dictates that the polymer extension grows as f^γ with force, f, for a self-avoiding chain in the regime $f \lesssim k_BT/\ell$. Direct measurement of γ in a single-molecule experiment has been accomplished;[6] however, there is not a full understanding of the experimental conditions and their potential effects in biasing estimates of γ. One key issue is the effect of surfaces. Surfaces are an unavoidable component of magnetic tweezer experiments, as the polymer under study must be attached at both ends to mechanically rigid points [typically a glass surface and paramagnetic bead; see Fig. 1(a)].

We explore the effect of surfaces in biasing experimental estimates of γ. Our focus is on a method of estimating γ from single-polymer extension fluctuations.[3,7] We show that this method leads, at very low forces, to an unexpected decrease in the γ estimate in measurements of both hyaluronic acid (HA) and poly(ethylene glycol) (PEG) chains. To explain this decrease, we formulate a model permitting an estimate of the effect of both surfaces in restricting the available configurations of a chain under tension. The calculation replicates the observed low-force decrease in γ and predicts that the decrease begins when the external force is $\approx 3k_BT/R_g$, where R_g is the chain's radius of gyration. This prediction is validated through comparison with the PEG and HA data. We show that estimates

[a)]S. N. Innes-Gold and I. L. Morgan contributed equally to this work.
[b)]Electronic mail: saleh@ucsb.edu

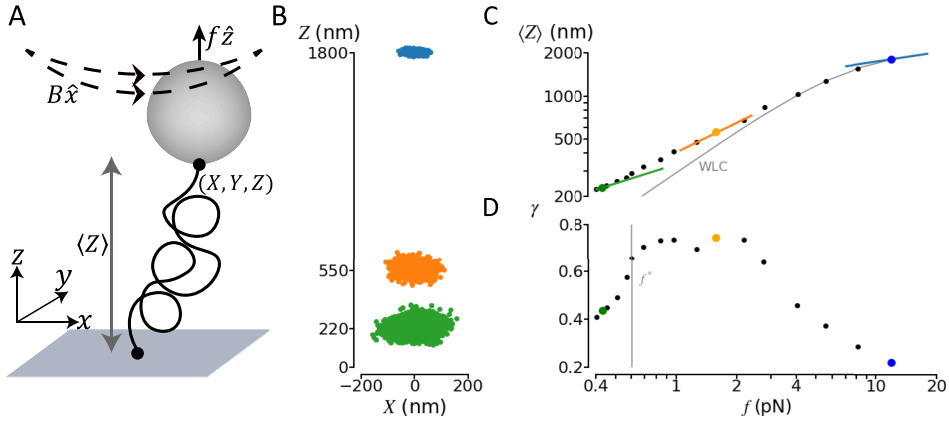

FIG. 1. (a) Sketch of magnetic tweezer experimental geometry: A paramagnetic bead subject to a field B oriented in $\hat{x}$, but with a gradient in $\hat{z}$, feels a force $f\hat{z}$, stretching the attached polymer. (b) Typical experimental measurement of fluctuating bead position for three representative constant forces: 12 pN (blue; 895 points), 1.6 pN (orange; 2175 points), and 0.42 pN (green; 7743 points), on a tethered PEG chain. (c) Black dots: absolute extension, $\langle Z\rangle$, vs. f curve for the same PEG chain as in panel (b). Colored lines indicate estimates of local power-law slope, γ, resulting from applying Eq. (1b) to the measured fluctuations for the three representative forces. The gray line is a fit of the worm-like chain elastic function to the high-force ($f > 4$ pN) data, returning $L_0 = 2900$ nm and $l_p = 0.6$ nm. (d) Full curve of γ vs. f for the same PEG tether, showing a downturn for forces below $f^* = 0.6$ pN.

of R_g based on the decrease in γ are consistent with those generated from knowledge of microscopic polymer parameters, themselves gleaned from other parts of the force-extension curve.

II. FLUCTUATION ESTIMATES OF POLYMER ELASTICITY

Resolving power-law exponents by direct fitting to sections of extension/force curves is difficult, as it is not clear which points are fully within a given regime and which are affected by neighboring regimes. Further, in the low-force regime, absolute extension becomes very small, leading to sensitivity to systematic errors based on, e.g., the precise tethering position of the polymer to the probe.[8,9] An alternate approach is based on the analysis of the fluctuations in polymer extension.[3,7] The fluctuation-based method is an application of linear response theory[10] and is discussed in detail elsewhere.[3] We consider a force oriented in the $\hat{z}$ direction that leads to a mean extension $\langle Z\rangle$ of the chain [see Fig. 1(a)]. Assuming a power-law elastic relation $\langle Z\rangle \sim f^{\gamma}$, the effective exponent in the vicinity of force f can be estimated from

$$\gamma(f) = \frac{f\,\mathrm{var}(Z)_f}{k_B T\,\langle Z\rangle_f} \tag{1a}$$

$$= \frac{\mathrm{var}(Z)_f}{\mathrm{var}(X)_f}, \tag{1b}$$

where var indicates the variance of a parameter about its mean, and Eq. (1b) adjusts Eq. (1a) by substituting the pendulum physics result for lateral thermal fluctuations, $\mathrm{var}(X) = k_B T\,\langle Z\rangle / f$, as is commonly applied for magnetic tweezer experiments.[11] We use the lateral fluctuations in the direction of the magnetic field (here, $\hat{x}$; see Fig. 1) to avoid the significant confounding effect of extra fluctuations due to bead rotational motion in $\hat{y}$.

Equation (1b) does not rely on knowledge of the mean extension of the chain. Thus, the resulting exponent estimate is independent of that found from the force-extension curve. Further, measurement of $\mathrm{var}(Z)$ and $\mathrm{var}(X)$ is robust since it relies on sensing large changes in the relative position of the bead, which is insensitive to the systematic errors in measuring $\langle Z\rangle$. Experimental application of Eq. (1b) results in a fluctuation estimate of the slope that matches the direct force-extension curve at moderate and high forces [Figs. 1(c) and 1(d)]. The estimated γ is consistent with 2/3 at moderate force before decreasing as the chain extension approaches its contour length.

At lower forces, the fluctuation estimate of γ clearly decreases; however, it is difficult to judge if this downturn agrees with the direct force-extension curve. Further, this downturn does not match simple theoretical expectations at low force, which predicts γ would increase from 2/3 to 1 in the lowest force linear-elastic regime.[3,12]

III. MODEL OF POLYMER/SURFACE INTERACTIONS

The major goal of this paper is to explain the low-force downturn in γ observed in Fig. 1(d). We postulate that it is caused by polymer/surface interactions, particularly the exclusion of the monomers from the volume occupied by the two tethering surfaces. Indeed, in this situation, at very low forces, one expects the chain extension to plateau near R_g, leading to an incompliant state that would decrease γ.[13] However, in the experimental data, the γ downturn is clear at extensions much larger than R_g. For example, for the PEG chain shown in Fig. 1, the downturn is clear at $\langle Z\rangle \approx 300$ nm, while we estimate that this chain has a much smaller value of $R_g \approx 43$ nm. The R_g estimate is found from the best-fit contour length, $L_0 = 2900$ nm, and using prior estimates of 0.278 nm contour length per PEG monomer,[14] the monomer molecular weight of 44 Da, and the relation of R_g to PEG molecular weight M_w, $R_g = 0.0215 M_w^{0.583}$, found from light scattering measurements.[15]

To test whether polymer/surface interactions can explain the γ downturn, we formulate a model of the surface's effect on the polymer configurational distribution. We use the image principle to estimate the number of allowed configurations

of an ideal random-walk chain in the presence of a surface.[16–18] The experimental chains are non-ideal, as shown by the swollen-chain ($\gamma \approx 2/3$) behavior at moderate elasticity (Fig. 1); however, the swollen-chain behavior is significantly more difficult to analyze. We thus focus on a tractable ideal-chain model, with the goal of testing whether the surface effect can indeed decrease γ at relatively large chain extensions.

When applied to a single excluded surface,[16] the image method gives the statistical weight (proportional to the number of allowed configurations), $G_{1S}(\vec{R},\vec{R}')$, of an ideal chain tethered at position $\vec{R}$ to a planar surface (taken to be the $z = 0$ plane) and whose opposite end is free and located at $\vec{R}'$,

$$G_{1S}(\vec{R},\vec{R}') = e^{-\frac{(X-X')^2}{4R_g^2}} e^{-\frac{(Y-Y')^2}{4R_g^2}} \left(e^{-\frac{(Z-Z')^2}{4R_g^2}} - e^{-\frac{(Z+Z')^2}{4R_g^2}} \right). \quad (2)$$

Here, the subtraction removes forbidden configurations (i.e., those that would intersect with the surface) from the ensemble of free chains (i.e., the permitted chain configurations in the absence of the surface). The Gaussian form of Eq. (2) enforces an infinitely extensible polymer; this is unphysical, but consistent with our focus on low-force, low-extension behavior. It does lead to disagreement with experiment in the high-force regime, when the finite extension of the actual polymer is approached.

We rewrite Eq. (2) as $G_{1S}(\vec{R},\vec{R}') = G_{free}(\vec{R},\vec{R}')(1 - p_{1S}(\vec{R},\vec{R}'))$, where G_{free} is the statistical weight of an unconstrained chain and p_{1S} is the probability that a member of the unconstrained ensemble will follow a forbidden path, given by

$$p_{1S}(\vec{R},\vec{R}') = e^{-ZZ'/R_g^2}. \quad (3)$$

We must account for two surfaces since, in the experiment, the chain is tethered to both a planar surface and a spherical bead. Since the bead radius (≈525 nm) is much larger than R_g, we treat it as a second planar surface, parallel to the first. This situation is entirely symmetric with respect to the two surfaces, which means that p_{1S} is the same for each surface individually. We then posit that $(1-p_{1S})^2$ is a good estimate for the probability that a member of the unconstrained ensemble will not intersect either surface. This estimate assumes that there is no correlation in the chance of intersection between the two surfaces. In reality, there is likely some correlation—particularly, the probabilities are likely anti-correlated, since a path that loops back to intersect one surface has less contour available to reach the other surface. However, we assume here that this is a small effect.

The statistical weight in the presence of both surfaces is then

$$G_{2S}(\vec{R},\vec{R}') = G_{Free}(\vec{R},\vec{R}') \left(1 - p_{1S}(\vec{R},\vec{R}')\right)^2. \quad (4)$$

To apply the image method to a tethered polymer, the terminus is fixed at a small distance, d, from the tethering surface;[16] this accounts for the unique chemical ability of the functional group to bind to the surface in a position disallowed to the monomers. So, for surface separation Z, the end monomers are located at $\vec{R}_1 = (0,0,d)$ and $\vec{R}_2 = (X,Y,Z-d)$. Further, we include the effect of force by weighting each configuration by the Boltzmann factor of the work done by the system, e^{fZ/k_BT}. Thus, the partition function for the system is

$$\mathcal{Z} = \int_{-\infty}^{\infty} dX \int_{-\infty}^{\infty} dY \int_{0}^{\infty} dZ e^{fZ/k_BT} G_{2S}(\vec{R}_1,\vec{R}_2), \quad (5)$$

where the bounds of the integrals reflect the bead's ability to move laterally, but its inability to pass through the glass surface. While Eq. (5) can be analytically integrated, the result is quite complex. In practice, we work with an approximate form of $\mathcal{Z}$, taken in the $d/R_G \ll 1$ limit, where the dependence on d drops out of the results.

We calculate ensemble average quantities of the parameters of interest, $\langle Z\rangle$, $\langle Z^2\rangle$, and $\langle X^2\rangle$, from the partition function, Eq. (5), in the small d limit. We set $\mathrm{var}(Z) = \langle Z^2\rangle - \langle Z\rangle^2$. Note that $\mathrm{var}(X) = \langle X^2\rangle = 2R_g^2$ for all forces. The model prediction for γ is found as the ratio of variances, per Eq. (1b).

IV. RESULTS AND COMPARISON TO DATA

The model produces the expected entropic-spring behavior, $\langle Z\rangle = 2R_g^2 f/k_BT$, for an ideal chain in the high-force limit [Fig. 2(a)]. Similarly, in Fig. 2(b), we see that the model's estimate of the variance ratio results in the expected value, $\gamma = 1$, in the high-force limit. For an unconstrained ideal chain, linear behavior should persist to low forces (dashed lines in Fig. 2). By contrast, the model prediction for γ shows a downturn [Fig. 2(b)], in qualitative agreement with experiment [Fig. 1(d)]. At a similar force, the force-extension curves show

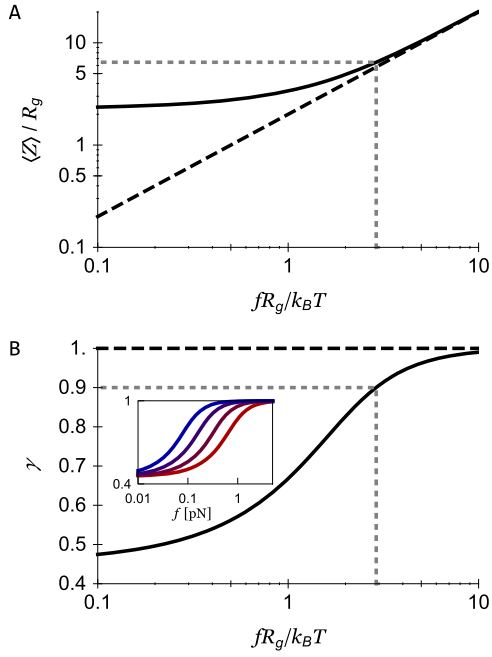

FIG. 2. (a) Dimensionless extension vs. force relation computed from the model for an ideal chain tethered between two parallel planar surfaces (solid line), compared with that of an unconstrained entropic spring (dashed line). (b) γ vs. dimensionless force computed from the model using Eq. (1b) (solid line), compared with the unconstrained entropic spring expectation $\gamma = 1$ (dashed line). In both panels, the coordinates at which $\gamma = 0.9$ are emphasized with dashed gray lines. Inset of panel (b): γ vs. absolute force for chains with (right to left) $R_g = 10$, 20, 40, and 80 nm.

a transition to a regime where $\langle Z \rangle$ is independent of force. By approximating the partition function, we find the predicted low-force limiting values: $\lim_{f\to 0}\langle Z\rangle = 4R_g/\sqrt{\pi} \approx 2.26R_g$ and $\lim_{f\to 0}\gamma = 3 - (8/\pi) \approx 0.45$. The latter estimate is similar to the variance ratio estimated from simulations of self-avoiding chains constrained by tethering to a single surface.[19]

The calculated surface-induced decrease in γ occurs at a force that scales with k_BT/R_g, as suggested based on inspection of the form of the partition function. The dependence on R_g is made explicit in the inset of Fig. 2, which shows γ versus absolute f (in piconewtons) for a range of R_g values. As shown, the downturn moves to higher forces as R_g decreases.

While the location of the predicted γ downturn scales with k_BT/R_g, the actual predicted location has a greater-than-unity multiplicative prefactor in both force and length. We judge the downturn as having begun when the γ value decreases by about 10% (this is when it is experimentally visible, as shown by the placement of f^* in Fig. 1). The model predicts that when $\gamma = 0.9$, the force is $2.9k_BT/R_g$, and the extension is $6.5R_g$; these values are indicated by the dashed gray lines in Fig. 2.

To gain more insight into the actual location of the downturn and to confirm experimentally whether k_BT/R_g is the controlling force scale for the γ downturn, we turn to a broad set of single-molecule data. In particular, we analyzed 44 force-extension curves acquired from single chains of PEG and 43 curves acquired from single chains of HA (details on experimental methods, and an example HA data set, Fig. S1, are available in the supplementary material). For the polyelectrolyte HA, data were acquired over a range of salt concentrations, which tunes the effective Kuhn length of the chain.[20] We apply Eq. (1b) to the data, generating a γ vs. f curve, and then estimate f^* from the observed low-force downturn [as in Fig. 1(d)].

We separately estimate the chain Kuhn length ℓ and number of Kuhn monomers $N = L_0/\ell$ by fitting the high-force portion of the $\langle Z \rangle$ vs. f curve to the worm-like chain (WLC) elasticity function[21,22] [see Fig. 1(c)] and setting $\ell = 2l_p$, where l_p is the best-fit persistence length. Across all chains, the PEG fits gave $\langle \ell \rangle = 1.3$ nm with a standard deviation of 0.2 nm and L_0 ranging from 940 nm to 6300 nm; the HA data had ℓ ranging from 7.6 nm to 17.8 nm and L_0 ranging from 800 to 5400 nm. The observed variation of the contour length is consistent with the polydisperse samples that were used.

Both PEG and HA form higher-order structures due to hydrogen bonding between neighboring monomers and/or between monomers and water.[9,14,23] High forces have been shown to disrupt these interactions,[9,14,24] which leads to deviations from WLC behavior, and can lead to elasticity-based estimates of l_p that are smaller than l_p in the absence of force. This issue is minimized here: those prior observations are based on AFM studies at a force scale of ≈100 pN. Here, our l_p estimates are based on fits at a much lower force scale (1–10 pN), where force-induced structural changes are a minor effect. Thus, we expect our WLC fit parameters to be a good estimate of low-force (<1 pN) polymer structure.

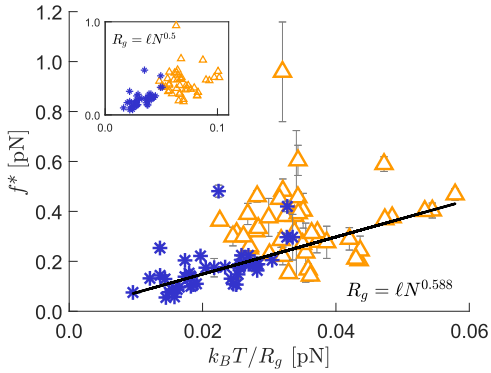

FIG. 3. Experimental correlation of f^* with k_BT/R_g for single polymers of HA (blue stars) and PEG (orange triangles). f^* is estimated from the low-force downturn in the fluctuation estimate of γ [see Fig. 1(d)], and R_g is estimated from the parameters extracted from high-force WLC fits [see Fig. 1(c)], with $\ell = 2l_p$ and $N = L_0/\ell$. The HA and PEG data show better overlap when using self-avoiding estimates of R_g (main plot) rather than ideal estimates (inset). The self-avoiding data are well-fit by a line passing through the origin, with slope 7.4 ± 0.3. Error bars reflect the discrete sampling of force and/or an intrinsic 5% uncertainty in force calibration.

We find that in the experimental data, k_BT/R_g indeed controls f^*, with a smooth dependence across both HA and PEG data sets seen if R_g is estimated from a scaling relation as $R_g = \ell N^{0.588}$. Using this self-avoiding approximation leads to a substantial overlap between the HA and PEG data, with f^* linearly increasing with k_BT/R_g (Fig. 3). Using the ideal relation $R_g = \ell N^{1/2}$ results in little overlap between the PEG and HA data (inset, Fig. 3).

To more quantitatively compare the data and model, we focus on PEG, for which Devanand and Selser (DS)[15] provide a relation between chain molecular weight and radius of gyration. We calculate molecular weight for each PEG chain from the best-fit L_0 value, as described above, and apply their formula to find $R_{g,DS}$; the resulting values are tightly correlated with the scaling estimate (see Fig. S2 of the supplementary material) but have the advantage of using a known numerical prefactor. Applying this radius of gyration estimate, we then calculate the value of the rescaled force and length at downturn across all 44 PEG curves, finding $\text{Mean}(f^*R_{g,DS}/k_BT) = 3.3 \pm 1.3$ and $\text{Mean}(\langle Z(f^*)\rangle/R_{g,DS}) = 4.0 \pm 1.4$ (the weighted mean is used for f^* and errors are given as the standard deviation). The large variation in each value across the population occurs because our ability to resolve f^* from the PEG data is somewhat error prone (as seen in Fig. 3) due to low-force noise in γ. However, the greater-than-unity value of both parameters qualititatively confirms the model predictions and quantitatively match well in the case of f^*, where the model predicted $f^*R_g/k_BT = 2.9$. The match is less good for rescaled length, where the model predicted $\langle Z(f^*)\rangle/R_g = 6.5$. This could be due to deficiencies in the model (notably its focus on ideal, rather than more realistic swollen chains) or due to aforementioned systematic experimental issues in estimation of small absolute extensions.

V. DISCUSSION

Our results confirm and illuminate the initial hypothesis: At low stretching forces, polymer extensional fluctuations

become cut off by exclusion from the tethering surface, decreasing the variance of the extensional distribution and leading to the downturn in γ seen in Fig. 1(d). Our image-based model of the effect of the surface captures this behavior [Fig. 2(b)], and analysis of the model predicts that the force, f^*, at which γ decreases by 10% is given by $f^* \approx 3k_BT/R_g$. From a scaling viewpoint, experimental validation is demonstrated by the linear variation of the measured force at downturn, f^*, with independent experimental estimates of k_BT/R_g for two types of chains (HA and PEG), and over a wide range of contour and Kuhn lengths (Fig. 3). Quantitatively, our measurements of PEG, for which R_g can be reliably independently estimated, indicate $f^*R_g/k_BT \approx 3.3$, in relatively good agreement with the model predictions.

Certain prior studies[3,12] predict that in the absence of a surface, the compliance of a self-avoiding chain would increase as tension decreases through k_BT/R_g. The observed γ downturn, corresponding to a decrease in chain compliance, occurs at the same scale, obscuring the predicted compliance-increase effect. Our results are consistent with the work of Neumann,[13] who discussed a plateau $\langle Z \rangle \approx R_g$ as $f \to 0$, as occurs in our calculation [Fig. 2(a)]. But, we do not clearly observe that plateau in experiment [Fig. 1(c)] due to the small values of $\langle Z \rangle$ and potentially due to confounding systematic errors. By contrast, the measured transition in γ is more clear [Fig. 1(d)], indicating that in the low-force limit, variance-based metrics are more sensitive probes of elasticity than absolute extension.

The transition measured here joins a variety of other elastic transitions that occur when stretching single polymer chains. These include the transition from random-walk to straight chain behavior,[3,12] at $f \sim k_BT/\ell$; the transition from WLC to freely-jointed chain behavior that occurs at $f \sim k_BT/b$, where b is the bond length;[25] and the emergence of excluded volume for rod-like chains, occurring below $f \sim k_BTv/\ell$,[4] where v is the monomer-level excluded volume parameter.[26,27] A major difference of the present transition is its sensitivity to the chain contour length: the other transitions only depend on intensive, microscopic polymer parameters such as the Kuhn or bond length. Thus, given two chains of identical composition, but different lengths, all transitions except the γ downturn will occur at the same forces. Indeed, this is directly demonstrated here in our analysis of experimental data (Fig. 3).

A remaining puzzle is to understand the behavior of γ in the zero-force limit. The model presented here relies on both the linear-response theory and the pendulum approximation to calculate γ through the application of Eq. (1b) and predicts a plateau in γ in the zero-force limit [Fig. 2(b)]. In preliminary work, we have instead explored directly applying Eq. (1a), which is still a linear-response result, but does not make the pendulum approximation. In that case, we still find a downturn in γ below k_BT/R_g. However, when using Eq. (1a), γ decreases continuously at low forces, rather than reaching a plateau. This disagreement points to an issue with the pendulum approximation in the presence of a surface and at low forces; more work is required to understand this aspect.

VI. CONCLUSION

We have shown that fluctuation-based estimates of polymer elasticity are sensitive to surface effects for forces below k_BT/R_g. An elastic transition at that scale was indeed anticipated by prior studies;[3,12] however, this work clarifies that in the presence of surfaces, the experimental signature of this transition is a *decrease*, rather than an increase, in chain compliance. The ability to observe this transition in a magnetic tweezer experiment means it is possible to independently estimate both R_g (from f^*) and N and ℓ (from high-force fitting) from a single measured force-extension curve. This broadens the capabilities of single-molecule manipulation instruments.

SUPPLEMENTARY MATERIAL

See supplementary material for details on polymer synthesis and data analysis.

ACKNOWLEDGMENTS

We gratefully thank Christina G. Rodriguez and Nathaniel A. Lynd (University of Texas, Austin) for the gift of the PEG polymer. O.A.S. thanks the Alexander von Humboldt Foundation for support. This work was supported by NSF Grant Nos. DMR-1611497 and MCB-1715627.

[1] M. S. Kellermayer, S. B. Smith, H. L. Granzier, and C. Bustamante, Science **276**, 1112 (1997).
[2] D. R. Jacobson, D. B. McIntosh, M. J. Stevens, M. Rubinstein, and O. A. Saleh, Proc. Natl. Acad. Sci. U. S. A. **114**, 5095 (2017).
[3] O. A. Saleh, J. Chem. Phys. **142**, 194902 (2015).
[4] K. C. Neuman and A. Nagy, Nat. Methods **5**, 491 (2008).
[5] P. Pincus, Macromolecules **9**, 386 (1976).
[6] O. A. Saleh, D. B. McIntosh, P. Pincus, and N. Ribeck, Phys. Rev. Lett. **102**, 068301 (2009).
[7] D. B. McIntosh, G. Duggan, Q. Gouil, and O. A. Saleh, Biophys. J. **106**, 659 (2014).
[8] D. Klaue and R. Seidel, Phys. Rev. Lett. **102**, 028302 (2009).
[9] S. Liese, M. Gensler, S. Krysiak, R. Schwarzl, A. Achazi, B. Paulus, T. Hugel, J. P. Rabe, and R. R. Netz, ACS Nano **11**, 702 (2016).
[10] L. D. Landau and E. M. Lifshitz, *Statistical Physics, Course of Theoretical Physics* (Elsevier, 1980), Vol. 5.
[11] T. R. Strick, J.-F. Allemand, D. Bensimon, A. Bensimon, and V. Croquette, Science **271**, 1835 (1996).
[12] R. R. Netz, Macromolecules **34**, 7522 (2001).
[13] R. M. Neumann, J. Chem. Phys. **110**, 7513 (1999).
[14] F. Oesterhelt, M. Rief, and H. Gaub, New J. Phys. **1**, 6 (1999).
[15] K. Devanand and J. Selser, Macromolecules **24**, 5943 (1991).
[16] T. Bickel, C. Jeppesen, and C. Marques, Eur. Phys. J. E **4**, 33 (2001).
[17] E. Eisenriegler, *Polymers Near Surfaces: Conformation Properties and Relation to Critical Phenomena* (World Scientific, 1993).
[18] J. Rudnick and G. Gaspari, *Elements of the Random Walk: An Introduction for Advanced Students and Researchers* (Cambridge University Press, 2004).
[19] R. Bubis, Y. Kantor, and M. Kardar, Europhys. Lett. **88**, 48001 (2009).
[20] J. P. Berezney and O. A. Saleh, Macromolecules **50**, 1085 (2017).
[21] C. Bouchiat, M. Wang, J.-F. Allemand, T. Strick, S. Block, and V. Croquette, Biophys. J. **76**, 409 (1999).
[22] J. F. Marko and E. D. Siggia, Macromolecules **28**, 8759 (1995).
[23] A. Almond, A. Brass, and J. Sheehan, J. Phys. Chem. B **104**, 5634 (2000).
[24] M. I. Giannotti, M. Rinaudo, and G. J. Vancso, Biomacromolecules **8**, 2648 (2007).
[25] A. V. Dobrynin, J.-M. Y. Carrillo, and M. Rubinstein, Macromolecules **43**, 9181 (2010).
[26] A. Dittmore, D. B. McIntosh, S. Halliday, and O. A. Saleh, Phys. Rev. Lett. **107**, 148301 (2011).
[27] D. Schaefer, J. Joanny, and P. Pincus, Macromolecules **13**, 1280 (1980).